ARCHIVES OF ELECTRICAL ENGINEERING VOL. 68(4), pp. 803–815 (2019)

DOI 10.24425/aee.2019.130684

Improved carrier phase shift modulation and voltage equalization control strategy in modular multilevel converter

HONGTAO JIN, YINGHONG LUO, YUHENG FAN, SHENGXIONG PAN

School of Automation and Electrical Engineering, Lanzhou Jiaotong University
China
e-mail: 719011448@qq.com

(Received: 05.05.2019, revised: 12.06.2019)

Abstract: In order to solve the problem of traditional carrier phase-shift modulation with multiple ratios or PI controllers and cumbersome tuning parameters, this paper uses improved carrier phase-shift modulation. The total turn-on number of sub-modules each bridge arm is determined by comparing the sinusoidal modulated wave with the triangular carrier, and then the control signal is generated according to the capacitance voltage sorting result and the bridge arm current polarity. However, this modulation method uses a sorting method that causes the insulated gate bipolar transistor (IGBT) have an excessively high switching frequency. Therefore, a sorting trigger condition that can effectively reduce the switching frequency is used. The method determines whether to reorder based on the error between the voltage average and the actual value. For the circulation problem, the double-frequency negative sequence component is extracted by rotating coordinate transformation, and it is suppressed by PI control. A 21-level MMC model was built in MATLAB/simulink to analyze the sub-module capacitor voltage fluctuation, output current, voltage distortion rate and bridge arm circulation. It is verified that the modulation method can combine the sorting algorithm and circulation suppression method at the same time, and has better voltage equalization and circulation suppression effects.

Key words: circulation suppression, modular multilevel converter, improved carrier phase shifting, switching frequency, voltage equalization

1. Introduction

A modular multilevel converter (MMC) has a modular structure. The sub-module series can increase the voltage level and voltage output quality, reduce the requirements on the AC side filter, and even achieve needed results with no filter. The MMC is widely used in medium and

© 2019. The Author(s). This is an open-access article distributed under the terms of the Creative Commons Attribution-NonCommercial-NoDerivatives License (CC BY-NC-ND 4.0, https://creativecommons.org/licenses/by-nc-nd/4.0/), which permits use, distribution, and reproduction in any medium, provided that the Article is properly cited, the use is non-commercial, and no modifications or adaptations are made.

www.czasopisma.pan.pl PAN POLSKA AKADEMIA NAUK www.journals.pan.pl

high voltage power conversion sites [1], offshore wind farm grid-connected, hybrid flexible DC transmission systems and two-terminal, multi-terminal flexible DC transmission systems [2, 3]. Once proposed, many scholars have done a lot of research on topological structure, modulation [4, 5], circulation suppression [6, 7], voltage equalization [8, 9], and sorting the algorithm [10–14]. Since the sub-module capacitor voltage fluctuation directly affects the MMC output voltage, current quality, and the overcharge as well as overdischarge of the capacitor that affects the capacitor life, the MMC sub-module capacitor voltage equalization control is extremely important.

In [15], the root cause of the double-frequency circulation when using the nearest level modulation is analyzed. The proposed voltage actual value approximation modulation strategy can effectively suppress the circulation, but this method is not suitable for the case of a small number of sub-modules. In [16], the frequency division and equalization control is proposed, so that the sorting frequency is much smaller than the control frequency, and the sorting frequency calculation process is derived, which can reduce the switching frequency and the computational burden. Literature [17] analyzes the necessary and sufficient conditions for the stability of the MMC system under open-loop control, and achieves voltage equalization by detecting the voltage of each bridge arm and injecting zero-sequence voltage. In [18], a new step-wave modulation method is proposed, which eliminates the need to measure the sub-module capacitance voltage and feedback control, so that the sub-module switch operates at the fundamental frequency and has a lower power loss. Literature [19] proposed a PI-controlled voltage equalization method, which has a certain weakening effect on the circulation, but the circulation suppression effect is not good. Literature [20] proposes a distributed voltage equalization, which distributes the voltage equalization controllers to each sub-module controller, which can reduce the computational burden of the central controller.

Nowadays, voltage equalization methods are mainly divided into two categories. One is a carrier phase shift combining ratio or PI control, and the other is the nearest level modulation combined with a sorting algorithm. Although the former can be combined with many circulation suppression methods, there are more proportions or PI controllers, and complex tuning parameters. Although the latter does not require a proportional or PI controller, the modulation method is not sensitive to the superposition of the weak circulation suppression control signal superimposed on the modulated wave, resulting in few circulation suppression methods being applied to the nearest level modulation. Therefore, this paper adopts improved carrier phase-shift modulation, which can combine a sorting algorithm and circulation suppression at the same time. It is not necessary to equip each sub-module with a proportional or PI controller. Only two PI controllers are needed for circulation suppression. And the method has better voltage stability and circulation suppression effect. For the problem that the IGBT switching frequency is too high caused by the sorting, the sorting trigger condition is used to control whether to reorder, which can effectively reduce the switching frequency.

2. MMC topology and basic principles

The topology of the modular multilevel converter is shown in Fig. 1. It consists of six bridge arms with n submodules and one inductor for each arm. Each submodule has the same structure and consists of two IGBTs and one capacitor. When T_1 or D_1 is turned on, it outputs the voltage U_c

www.czasopisma.pan.pl PAN POLSKA AKADEMIA NAUK www.journals.pan.pl

across the output capacitor; when T_2 or D_2 is turned on, it outputs 0. The upper and lower IGBT signals are opposite. The inductance of each bridge arm has a certain circulation suppression effect.

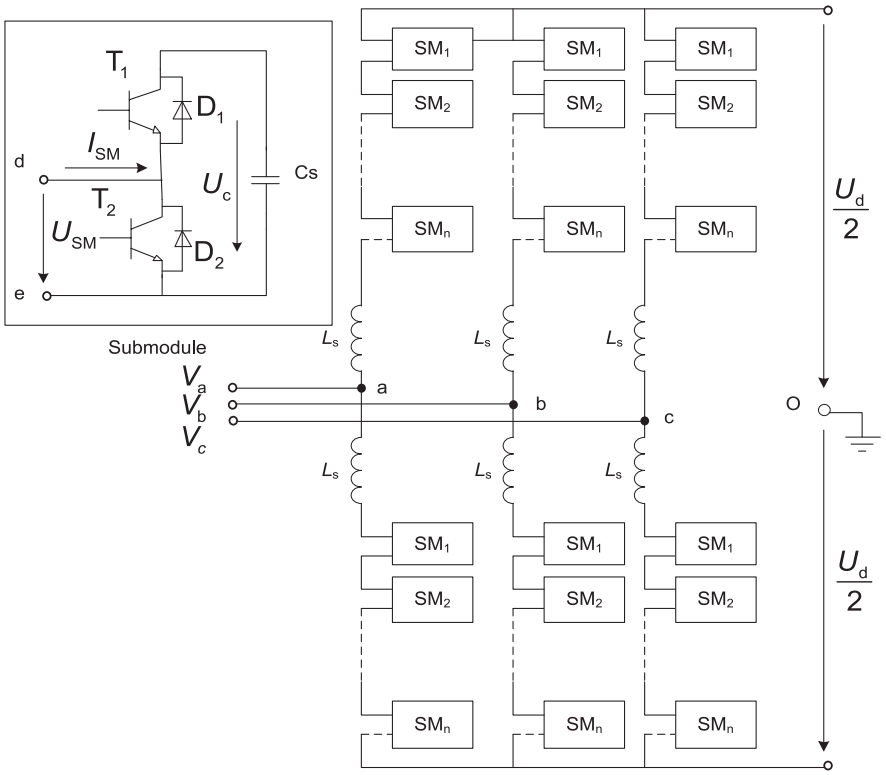

Fig. 1. Circuit topology of modular multilevel converter

The MMC single-phase equivalent circuit is shown in Fig. 2. The sub-modules of upper or lower bridge arm can be equivalent to a controlled voltage source. U_{up_a} is the equivalent output voltage of the upper arm, U_{down_a} is the equivalent output voltage of the lower arm, I_{loop_a} is the circulating current, I_{up_a} is the upper arm current, and I_{down_a} is the lower arm current. As shown in Equation (1), the upper and lower arm voltages are obtained by Kirchhoff's voltage law. A single-phase output voltage is shown in Equation (2). The circulation is shown in Equation (3).

$$\begin{cases} U_{up\_a} = \dfrac{U_d}{2} - U_{ao} \\ U_{down\_a} = \dfrac{U_d}{2} + U_{ao} \end{cases}, \tag{1}$$

$$\begin{cases} I_{up\_a} = I_{loop\_a} + \dfrac{I_a}{2} \\ I_{down\_a} = I_{loop\_a} - \dfrac{I_a}{2} \end{cases}, \tag{2}$$

www.czasopisma.pan.pl PAN POLSKA AKADEMIA NAUK www.journals.pan.pl

$$I_{\text{loop\_a}} = \frac{I_{\text{up\_a}} + I_{\text{down\_a}}}{2}. \tag{3}$$

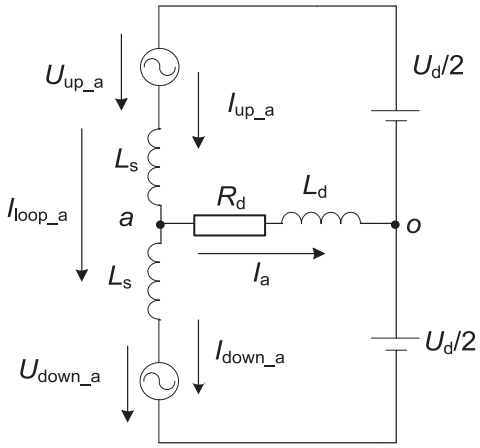

Fig. 2. Single-phase equivalent circuit diagram

3. Analysis of various modulation methods

3.1. Nearest level modulation and voltage equalization

The nearest level modulation is the most widely used method in engineering. Its control principle is simple, and suitable for applications requiring a large number of sub-modules. But if used in a small number of levels, the waveform quality is poor. The method approximates the modulated wave in the form of a step wave by superimposing the voltage of the sub-module capacitors. The voltage error between the modulated wave and step wave is within $\pm U_c/2$, and the number of sub-modules that are instantaneously turned-on in each phase unit is constant at N.

The number of sub-modules to be turned on at a certain moment is obtained by Equation (4), where N is the number of sub-modules of each bridge arm, n_{up} is the number of submodules to be turned on in the upper-arm, and n_{down} is the number of submodules to be turned on in the lower arm, U_r^* is the sinusoidal modulation signal, U_{ref} is the submodule capacitor voltage reference value, and *round* is the rounding function.

$$\begin{cases} n_{\text{up\_a}} = \dfrac{N}{2} - \text{round}\left(\dfrac{U_r^*}{U_{\text{ref}}}\right) \\ n_{\text{down\_a}} = \dfrac{N}{2} + \text{round}\left(\dfrac{U_r^*}{U_{\text{ref}}}\right) \end{cases}. \tag{4}$$

In this mode, the voltage equalization method firstly detects the actual value of the sub-module capacitor voltage of each bridge arm and sorts it. When the bridge arm current is positive, the capacitor of the turned-on sub-module is charged and the voltage rises. To maintain voltage balance, sub-modules with a low voltage are preferentially charged. Therefore, the voltage

values are sorted from low to high during sorting, and the sub-modules with low voltages are preferentially turned on. When the bridge arm current is negative, the capacitor of the turned-on sub-module discharges and the voltage drops. To maintain voltage balance, sub-modules with high voltages are preferentially discharged. Therefore, the voltage values are sorted from high to low during sorting, and the high voltage sub-modules preferentially conduct discharge.

But this method has the following problems:

1. The average switching frequency of the IGBT in the submodule is too high, and the MMC_HVDC system has a large loss. The solution mainly achieves the frequency reduction of the IGBT by improving the sorting algorithm and the reordering criterion.
2. The large number of sub-modules will result in heavy computational load and long calculation time. The solution mainly introduces various quick sorting ideas by improving the sorting algorithm, and reduces the time complexity of the algorithm.
3. The modulation method is not sensitive to the circulation control signal superimposed on the modulated wave, and thus few circulation suppression methods are applied to the nearest level modulation mode. The solution can only achieve the circulation suppression by superimposing the modulation wave on the actual value of the capacitor voltage.

3.2. Carrier phase-shift modulation and voltage equalization

The carrier phase shift modulation method has good performance in tracking modulated waves, and can significantly improve the output characteristics of the low level converter. However, as the number of levels increases, the method becomes more and more complicated, so it is generally used in low level applications. A pulse signal of the T_1 tube is generated by using n sets of bipolar triangular carriers whose phase is shifted by $2\pi/n$ and a three-phase sinusoidal modulation signal, and is inverted and sent to the T_2 tube. The sub-module carrier signals at the corresponding positions of the upper and lower arms are the same, and the upper and lower arm modulation waves are inverted.

As shown in Fig. 3, the actual measured capacitance voltage value U_{c_ai} is compared with the reference value U_c^* to generate a deviation. The proportional link is combined with the polarity of a bridge arm current to output the control signal U_{c_a1}, and finally superimposed on the modulated wave. In the assessment link of the polarity of bridge arm current, if it is the upper bridge arm sub-module, only the polarity of the I_{up} of the corresponding phase needs to be assessed. If it is the lower bridge arm sub-module, the polarity of the I_{down} of the corresponding phase only needs to be judged. Taking the upper bridge arm of the a-phase as an example, if $I_{up\_a} > 0$, output $+1$; if $I_{up\_a} < 0$, output -1.

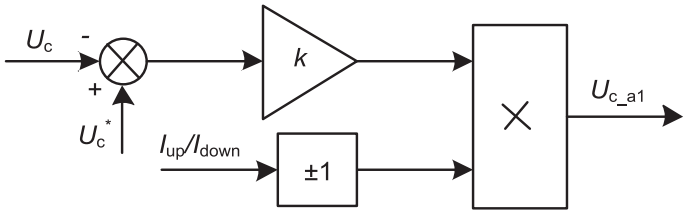

Fig. 3. Voltage balance control block diagram

www.czasopisma.pan.pl PAN POLSKA AKADEMIA NAUK www.journals.pan.pl

The voltage balance adjustment amount is as shown in Equation (5). When the bridge arm current is positive, the actual capacitor voltage U_c is lower than the set value U_c^*. The larger the deviation, the larger the adjustment amount, the longer the capacitor charging time, and the higher the voltage. The actual capacitor voltage U_c is higher than the set value U_c^*. The larger the deviation, the smaller the adjustment amount, the smaller the charging time of the capacitor, and the slower the voltage rise. The same can be analyzed in other situations.

$$U_{c\_a1} = \begin{cases} k(U_c^* - U_c), & I_{up\_a} > 0 \quad \text{or} \quad I_{down\_a} > 0 \\ -k(U_c^* - U_c), & I_{up\_a} < 0 \quad \text{or} \quad I_{down\_a} < 0 \end{cases}. \tag{5}$$

The method can be combined with several circulation suppression methods and has better circulation suppression effects, such as PI control, PR control, and the like. However, the voltage equalization method in the modulation mode has a cumbersome parameter adjustment process, and as the number of sub-modules increases, the system cost increases due to an increase in the number of proportional controllers.

3.3. The carrier phase-shift modulation and voltage equalization

The advantage of the improved carrier phase shift modulation method is that it does not require a large number of ratios or PI controllers, and because of its carrier phase shifting characteristics, its modulation wave tracking performance is better, this way it can be freely combined with various circulation suppression methods.

Fig. 4 is a flow chart of voltage equalization control with improved carrier phase shift modulation. A pulse width control signal is generated by comparing n sets of phase-shifted $2\pi/n$ bipolar triangular carriers with a three-phase sinusoidal modulated signal, and n sets of pulse width control signals are added to obtain the number of total turn-on sub-modules of each bridge-arm at a certain time. The number is n_{on}. The sub-module carrier signals of the upper and lower bridge arms are the same, and the upper and lower bridge arm modulation waves are inverted. Taking 20 sub-modules of a single bridge arm and a triangular carrier period of 5 ms as an example, the angle at which each group of triangular carriers is staggered is 18°, that is, the delay interval is 0.25 ms.

Among them, the average deviation limit assessment link has the effect of reducing the switching frequency of the sub-module. The method compares the voltage average with the actual value and sets an error tolerance range. If the limit is exceeded, the enable pulse lead in reordering, otherwise the original IGBT signal is maintained. This method can make the sub-modules that have been turned on preferentially, reduce the number of times of reordering and switching frequency. The judgment condition is as shown in Equation (6), U_{ci} is the sub-module capacitor voltage, U_{avg} is the average value of the capacitor voltage of each bridge arm, and i is the capacitance level of each bridge arm, and the value is $1, \ldots, n$, c is the set allowable error range.

$$\max\left\{\left|U_{ci} - U_{avg}\right|\right\} > c. \tag{6}$$

Determine whether the difference between the actual value of the sub-module voltage and the average value exceeds the limit and whether the number of the turn-on sub-modules changes. If one of the two conditions is satisfied, the sub-module capacitor voltage is reordered by the

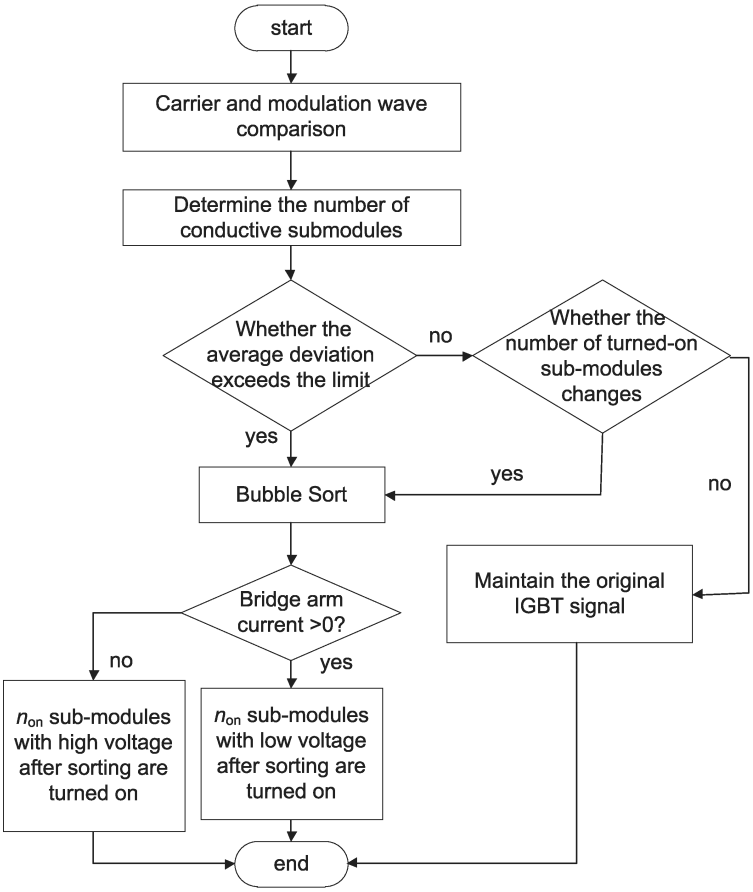

Fig. 4. Flow chart of voltage equalization control

sorting algorithm. Finally, a control signal is generated according to the voltage sorting result and the current polarity, and the pulse signal is sent to the T_1 tube and the pulse signal of the T_2 tube is inverted. The voltage equalization process is analyzed by taking the a-phase upper arm as an example. If $I_{up\_a} > 0$, the sub-modules of the bridge arm are in a charging state, and thenn_{on} sub-modules with low voltage after the sequencing are turned on. If $I_{up\_a} < 0$, the sub-modules of the bridge arm are in a discharging state, and the n_{on} sub-modules with high voltage after the sequencing are turned on.

4. Circulation analysis and suppression method

The voltage equalization control stabilizes the capacitor voltage of each sub-module near the rated value, but there is a slight voltage fluctuation. This causes the sum of the voltages of the upper and lower arms of the phases to be inconsistent with each other, resulting in an internal

circulation of the MMC, which flows only in the three-phase bridge arms, and has no effect on the external AC system.

The circulating components mainly have a direct current component and a double frequency negative sequence component. The internal current $I_{\text{loop\_}j}$ (j = a, b, c) of the three phases a, b, c is as shown in Formula (7). I_{dc} is the DC current, $I_{2\text{f}}$ is the double-frequency circulation peak, ω_0 is the fundamental angular frequency, and φ_0 is the initial phase angle.

The double-frequency negative sequence circulation is decomposed into two DC quantities by using a rotating coordinate transformation. Circulation suppression structure diagram is shown in Fig. 5. The three-phase circulation is obtained by Equation (3), and the cycloid dq component is obtained by the double-frequency negative-sequence rotation coordinate transformation. After comparing with the dq current command value, the dq reference values $u_{\text{diff d\_ref}}$ and $u_{\text{diff q\_ref}}$ of unbalanced voltage-drop are obtained by the PI, thus introducing the feedforward control to decouple. Finally, the three-phase negative-sequence unbalanced voltage drop reference value $u_{\text{diff }j\text{\_ref}}$ (j = a, b, c) is obtained through the inverse transform $\boldsymbol{T}_{\text{dq/acb}}$.

$$\begin{cases} I_{\text{loop\_a}} = \dfrac{I_{\text{d}}}{3} + I_{2\text{f}} \sin\left(2\omega_0 t + \varphi_0\right) \\ I_{\text{loop\_b}} = \dfrac{I_{\text{d}}}{3} + I_{2\text{f}} \sin\left(2\omega_0 t + \varphi_0 + \dfrac{2\pi}{3}\right) \\ I_{\text{loop\_c}} = \dfrac{I_{\text{d}}}{3} + I_{2\text{f}} \sin\left(2\omega_0 t + \varphi_0 - \dfrac{2\pi}{3}\right) \end{cases} . \tag{7}$$

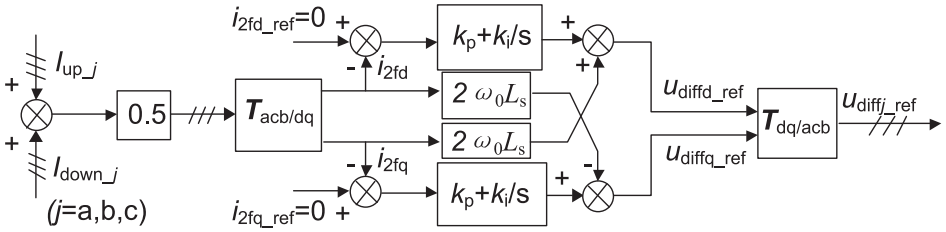

Fig. 5. Circulation suppression structure diagram

The overall control diagram of the MMC is shown in Fig. 6. A three-phase sinusoidal modulation signal is e_{j_ref}. After adding the circulation suppression control signal, the upper

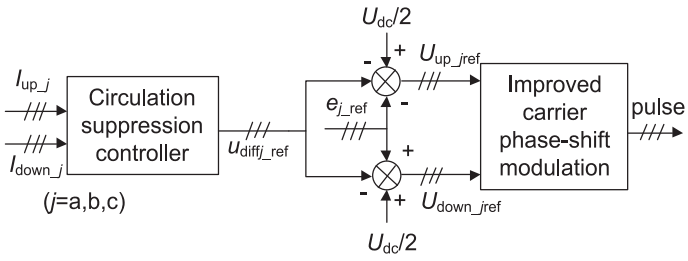

Fig. 6. MMC overall control charts

and lower arm voltage reference values $U_{\text{up\_}j\text{ ref}}$ and $U_{\text{down\_}j\text{ ref}}$ are finally output, and the trigger pulse is generated by using the improved carrier phase shift modulation to control the turn-on and turn-off of each sub-module.

5. Simulation and results

A 21-level MMC model was built in MATLAB/simulink to verify the voltage equalization and circulation suppression effects with improved carrier phase-shift modulation. The structure of the simulation circuit is shown in Fig. 7. The DC power supply $U_{\text{d}}/2$ is 20 kV, the load resistance R_{d} is 22 Ω, the load inductance L_{d} is 10 mH, the bridge arm inductance L_{s} is 4 mH, the bridge arm resistance is 0.1 Ω, the sub-module capacitance is 13 mF, and the sub-module voltage rating is 2 kV, the circulation suppression controller has a scale factor of 4 and an integral coefficient of 2 000.

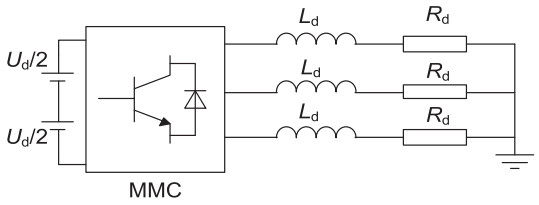

Fig. 7. Simulation circuit structure

Set the submodule capacitor initial voltage value to 2 kV. Before 0.3 s, only voltage equalization control is performed. After 0.3 s, circulation suppression is added. The capacitor voltage of all sub-modules on the a-phase upper arm is shown in Fig. 8. When the voltage is equalized, the stable voltage fluctuation is ±60 V, which is ±3% of the voltage rating. After the addition of the circulation suppression, the voltage fluctuation is ±40 V, which is ±2% of the voltage rating. The comparison shows that after the addition of the circulation suppression, the voltage fluctuation is further reduced and the voltage equalization effect is better. The interaction between voltage equalization and circulation suppression was verified.

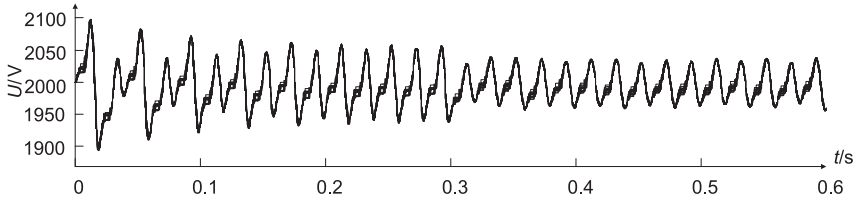

Fig. 8. Capacitor voltage of sub-modules

As shown in Fig. 9, the d, q axis current command value is set to 0, and the circulation suppression is added after 0.3 s. After 0.3 s, the d and q current quickly stabilized around zero. The a-phase circulation waveform and the harmonic analysis are respectively shown in Fig. 10

www.czasopisma.pan.pl PAN POLSKA AKADEMIA NAUK www.journals.pan.pl

and Fig. 11. Before 0.3 s, the DC component of the circulation is 220.2 A, and the second harmonic component is 84.77%. After the circulation is suppressed, the DC component of the circulation is 221.7 A, and the second harmonic component is 4.71%. The comparison shows that the second harmonic is changed from 84.77% to 4.71%, which is 80.06% lower. It is verified that the circulation suppression method has a good effect.

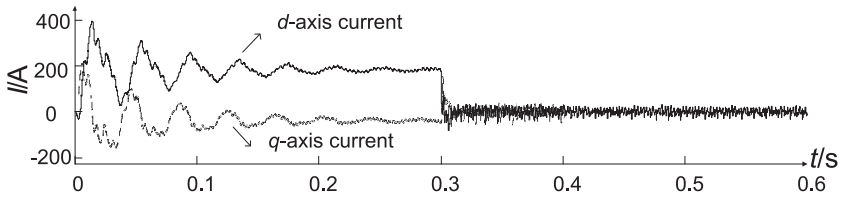

Fig. 9. d, q-axis current

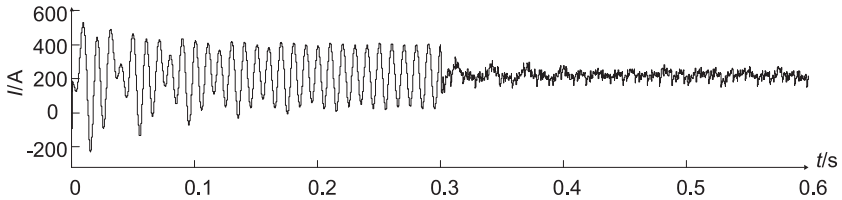

Fig. 10. a-phase circulation

Sampling time = 5e-05 s
Samples per cycle = 400
DC component = 220.2
Fundamental = 2.178 peak (1.54 rms)
THD = 84.97%

0 Hz (DC):	100.00%	90.0°
10 Hz	1.07%	263.9°
20 Hz	1.79%	246.3°
30 Hz	1.02%	83.9°
40 Hz	0.44%	-25.5°
50 Hz (Fnd):	0.99%	-73.1°
60 Hz	1.13%	-75.1°
70 Hz	3.49%	-88.6°
80 Hz	2.81%	135.1°
90 Hz	1.06%	123.9°
100 Hz (h2):	84.77%	79.9°
110 Hz	0.48%	119.2°
120 Hz	0.42%	109.3°
130 Hz	0.16%	153.4°
140 Hz	0.21%	136.3°
150 Hz (h3):	0.20%	128.9°
160 Hz	0.18%	129.3°
170 Hz	0.22%	117.9°
180 Hz	0.03%	109.8°
190 Hz	0.07%	139.4°
200 Hz (h4):	1.92%	258.8°
210 Hz	0.08%	142.5°
220 Hz	0.08%	146.6°

(a) Harmonic analysis before circulation suppression

Sampling time = 5e-05 s
Samples per cycle = 400
DC component = 221.7
Fundamental = 2.589 peak (1.831 rms)
THD = 13.23%

0 Hz (DC):	100.00%	90.0°
10 Hz	1.07%	129.5°
20 Hz	1.38%	168.0°
30 Hz	1.57%	200.2°
40 Hz	2.80%	33.6°
50 Hz (Fnd):	1.17%	80.8°
60 Hz	1.93%	136.2°
70 Hz	4.28%	112.3°
80 Hz	0.70%	-46.2°
90 Hz	0.76%	-4.9°
100 Hz (h2):	4.71%	-60.8°
110 Hz	1.66%	35.6°
120 Hz	0.19%	253.4°
130 Hz	0.56%	-26.8°
140 Hz	1.88%	-20.8°
150 Hz (h3):	1.84%	2.2°
160 Hz	0.84%	-4.3°
170 Hz	0.55%	59.8°
180 Hz	0.38%	-17.2°
190 Hz	0.66%	-69.6°
200 Hz (h4):	2.93%	3.8°
210 Hz	1.03%	39.1°
220 Hz	0.73%	30.1°

(b) Harmonic analysis after circulation suppression

Fig. 11. Circulation harmonic analysis

www.czasopisma.pan.pl PAN POLSKA AKADEMIA NAUK www.journals.pan.pl

The a-phase AC output voltage and current are shown in Fig. 12. After the circulation is suppressed, the voltage distortion rate decreases from 4.29% to 3.73%, and the current distortion rate decreases from 1.52% to 1.23%, which satisfy the condition that the distortion rate is less than 5%.

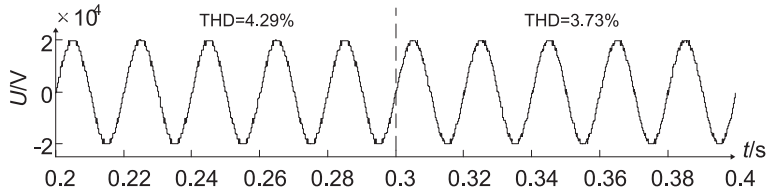

(a) A-phase output voltage

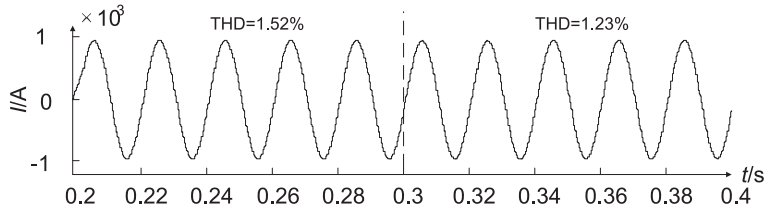

(b) A-phase output current

Fig. 12. a-phase AC output

The switching frequency of the IGBT is measured by triggering the cumulative counting of the rising edge pulse of the IGBT control signal. The IGBT control signals before and after reducing switching frequency are shown in Fig. 13. Before the addition of the reducing frequency control, the average switching frequency of the IGBT in the sub-module is measured to be 3553 Hz.

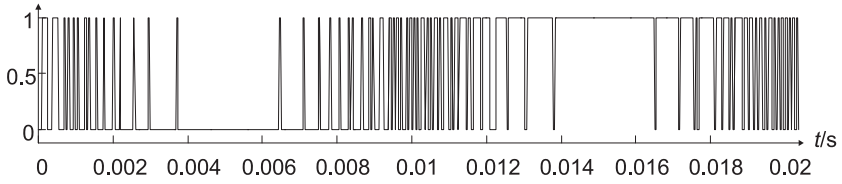

(a) Control signal of IGBT before frequency reduction control

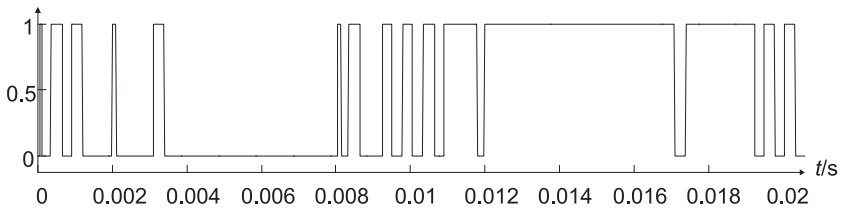

(b) Control signal of IGBT after frequency reduction control

Fig. 13. IGBT control signal

www.czasopisma.pan.pl PAN POLSKA AKADEMIA NAUK www.journals.pan.pl

After adding frequency control, the switching frequency is 614.1 Hz, which is 82.7% lower. This verifies the effectiveness of this method in reducing the switching frequency.

The voltage initial value of the sub-modules capacitor is set to 0. The rated voltage is 2 000 V. The dynamic response of the capacitor voltage is shown in Fig. 14. After 0.15 s, the capacitor voltage is stable at around 2 000 V. Therefore, the proposed control method has good dynamic response stability and no negative effect on the dynamic characteristics of the system.

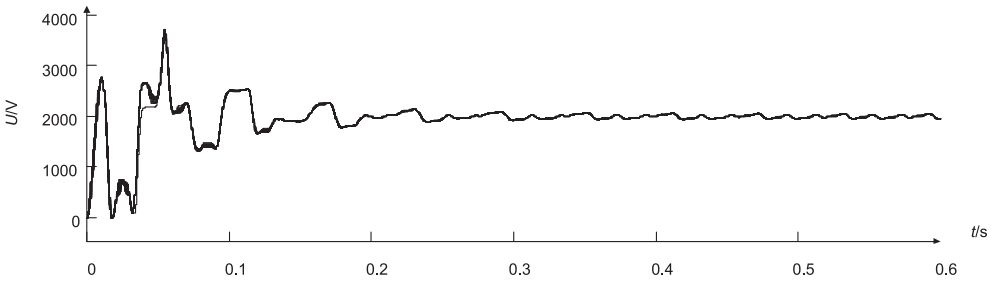

Fig. 14. Dynamic response of capacitor voltage

6. Conclusions

In this paper, the improved carrier phase shift modulation is used, which does not require a large number of proportional or PI controllers, and there is no complicated parameter tuning process. The method has better modulation wave following characteristics and can combine the sorting algorithm and the PI circulation suppression method at the same time. The voltage equalization control method can stabilize capacitor voltage very well. The circulation suppression method can effectively suppress the double-frequency negative-sequence circulation and make the capacitor voltage more stable. The reordering trigger condition can avoid unnecessary repeated switching of the IGBT and effectively reduce the IGBT switching frequency. The improved modulation method is suitable for medium and low voltage flexible DC transmission systems and has certain engineering application value.

References

[1] Xu Yijia, Luo Yinghong, Shi Tongtong *et al.*, *A new MMC sub-modules with DC fault self-clearing ability and its hybrid topology*, Power System Protection And Control, vol. 46, no. 7, pp. 129–137 (2018).

[2] Julian Freytes, Samy Akkari, Pierre Rault *et al.*, *Dynamic Analysis of MMC-Based MTDC Grids: Use of MMC Energy to Improve Voltage Behavior*, IEEE Transactions on Power Deliverys, vol. 34, no. 1, pp. 137–148 (2019).

[3] Li Guoqing, Wang Weru, Xin Yechun *et al.*, *Modular multilevel converter submodule packet sequencing modulation strategy*, High Voltage Technology, vol. 44, no. 7, pp. 2107–2114 (2018).

[4] Mohamed Moez Belhaouane, Mohamed Ayari, Xavier Guillaud *et al.*, *Robust Control Design of MMC-HVDC Systems Using Multivariable Optimal Guaranteed Cost Approach*, IEEE Transactions on Industry Applications, vol. 55, no. 3, pp. 2952–2963 (2019).

www.czasopisma.pan.pl PAN POLSKA AKADEMIA NAUK www.journals.pan.pl

[5] Sreedhar Madichetty, Abhijit Dasgupta, Sambeet Mishra *et al*., *Application of an Advanced Repetitive Controller to Mitigate Harmonics in MMC With APOD Scheme*, IEEE Transactions on Power Electronics, vol. 31, no. 9, pp. 58–68 (2016).

[6] Li Shanying, Wu Tao, Ren Bin *et al*., *Overview of energy storage systems based on modular multilevel converter*, Power System Protection and Control, vol. 43, no. 16, pp. 139–146 (2015).

[7] Firouz Badrkhani Ajaei, Reza Iravani, *Cable Surge Arrester Operation Due to Transient Overvoltages Under DC-Side Faults in the MMC–HVDC Link*, IEEE Transactions on Power Delivery, vol. 31, no. 3, pp. 1213–1222 (2016).

[8] Xue Hua, Li YangTang, Wang Yufei *et al*., *Passivity – based PI stability control and circulating current suppression method of MMC – HVDC [J]*, Power System Protection and Control, vol. 45, no. 19, pp. 78–85 (2017).

[9] Ricardo Vidal-Albalate, Hector Beltran, Alejandro Rolán *et al*., *Analysis of the Performance of MMC Under Fault Conditions in HVDC-Based Offshore Wind Farms*, IEEE Transactions on Power Delivery, vol. 31, no. 2, pp. 839–847 (2016).

[10] Yongjie Luo, Zixin Li, Luona Xu *et al*., *An Adaptive Voltage-Balancing Method for High-Power Modular Multilevel Converters*, IEEE Transactions on Power Electronics, vol. 33, pp. 2901–2912 (2018).

[11] Apparao Dekka, Bin Wu, Navid R. Zargari *et al*., *A Space-Vector PWM-Based Voltage-Balancing Approach with Reduced Current Sensors for Modular Multilevel Converter*, IEEE Transactions on Power Electronics, vol. 63, pp. 2734–2745 (2016).

[12] Apparao Dekka, Bin Wu, Navid R. Zargari *et al*., *Dynamic Voltage Balancing Algorithm for Modular Multilevel Converter: A Unique Solution*, IEEE Transactions on Power Electronics, vol. 31, pp. 952–963 (2016).

[13] Xiangdong Liu, Jingliang Lv, Congzhe Gao *et al*., *A Novel Diode-Clamped Modular Multilevel Converter With Simplified Capacitor Voltage-Balancing Control*, IEEE Transactions on Industrial Electronics, vol. 64, pp. 8843–8854 (2017).

[14] Apparao Dekka, Bin Wu, Ricardo Lizana Fuentes *et al*., *Voltage-Balancing Approach with Improved Harmonic Performance for Modular Multilevel Converters*, IEEE Transactions on Power Electronics, vol. 32, pp. 5878–5884 (2017).

[15] Zhang Jing, Hao Liangliang, Huang Yinhua *et al*., *Circulating Harmonic Suppressing Strategy for MMC Based on Superimposed Approach Modulation*, Power System Technology, vol. 41, no. 11, pp. 3539–3546 (2017).

[16] Hao Liangliang, Zhang Jing, Huang YinhuaXin *et al*., *Frequency dividing control of capacitor voltage balance for modular multilevel converter*, Electric Power Automation Equipment, vol. 38, no. 6, pp. 195–223 (2018).

[17] Xia Chaoying, Yu Jiali, *The Asymptotic Stability and Capacitor Voltage Balancing Control Strategy for MMC*, Proceedings of the CSEE, vol. 38, no. 19, pp. 5812–5821 (2018).

[18] Ni Shuangwu, Su Jianhu, Zhou Songlin, *MMC capacitance voltage balance strange based on fundamental switching frequency*, Acta Energiae Solaris Sinica 2017, vol. 38, no. 2, pp. 293–301 (2018).

[19] Ma Shang, Wang Yi, *Research on Capacitor Voltage Balancing Control Strategy of Modular Multilevel Converter*, Modern Electricity, vol. 34, no. 2, pp. 55–60 (2015).

[20] Li Jianguo, Yang Wenbo, Song Qiang *et al*., *Distributed equalization control method for modular multilevel converter capacitor voltage*, Automation of Electric Power Systems, vol. 40, no. 17, pp. 197–203 (2016).